RELAXATION OF HOT ELECTRONS IN SOLIDS OF REDUCED DIMENSIONS

R. PORATH, T. OHMS, M. SCHARTE, J. BEESLEY,
M. WESSENDORF, O. ANDREYEV, C. WIEMANN,
AND M. AESCHLIMANN
Department of Physics, University of Kaiserslautern
Erwin Schroedinger Str. 46, D-67663 Kaiserslautern

1. Abstract

The dynamics of optically excited electrons in solids of reduced dimensions is studied by means of time-resolved two-photon photoemission. In ultrathin films, the lifetime measurements show a clear change by the transition from bulk to layer dimensions smaller than the mean free path of the excited electrons. In silver nano-particles, the electron dynamics does not only depend on the reduced dimension of the systems but rather how the light is coupled into the system (on or off the Mie plasmon resonance). The later effect can be understood in terms of the increased radiation damping in nano-particles.

2. Introduction

A large variety of modern research fields such as fs-photochemistry and (magneto) electronics depend critically on the dynamics of photoexcited hot electrons. In recent years, the dynamics of optically excited electrons in metals, semiconductors and adsorbates has been investigated intensively, in particular by means of the time (and spin) resolved two-photon photoemission technique (TR-2PPE) [1-5]. These investigations have shown that electron dynamics depends critically on the excitation energy, the electron density of states, i.e. the band structure, as well as on the screening of the excited electrons (see Figure 1). As a consequence, the relaxation process of optically excited electrons in transition metals happens on times scales an order of magnitude faster than in noble metals [6]. Additionally, the influence of the spin polarization has been analysed for ferromagnets and semiconductors [4, 7].

The question arises how one can manipulate the lifetime of these hot electrons to design the electrodynamic properties for a specific application. In this paper it will be demonstrated that the specific structuring of the material on a nanometer scale can govern the effective electron dynamics. In order to tune the properties of optically

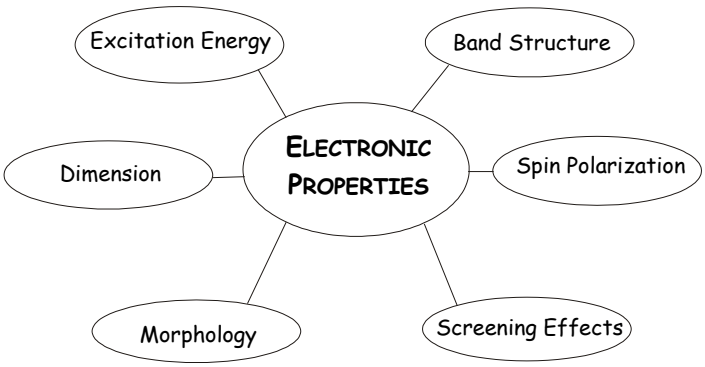

Figure 1. The electronic properties are influenced by different intrinsic (band structure, spin polarization, screening effects) and extrinsic (excitation energy, dimension, morphology) parameters.

excited electrons, we altered the dimensionality and morphology by using two different approaches: i) a reduction from a 3D-bulk to a 2D layered structure and ii) the preparation of defined nanoparticle geometries using the technique of electron beam lithography. By engineering the diameters, heights and the surrounding material the resonance frequency of involved Mie-plasmons can be changed, which considerably influence the electron dynamics.

3. Theory

3.1. THE TRANSITION TO LOWER DIMENSION

The dissipation processes of excited (hot) carriers in metals have been subject of intense theoretical work for several decades. Early theoretical approaches were based on the Landau theory of Fermi liquids (FLT), which treats the excitation as a quasiparticle. The lifetime τ_{ee} of a single particle excitation of an electron gas, as determined by electron-electron interactions, can be calculated from the imaginary part E_I of its self energy E(p), where p is the momentum of the excited electron. Quinn and Ferrell treated this problem in a theoretical study considering a Fermi liquid-like free electron gas [8, 9]. In the case of low excitation energies E(p), and when the effect of plasmon creation can be excluded ($E(p) << \omega_p$), they derived the following simple expression of the lifetime τ_{ee} in a 3D system which is known as Fermi-liquid behavior (FLT):

$$\tau_{ee}^{-1} = \tau_0^{-1} \cdot \left(E - E_F\right)^2 \tag{1}$$

The prefactor τ_0 is primarily determined by the free electron density n and is approximately given by [6]

$$\tau_0^{-1} \approx \frac{\sqrt{3}\cdot\pi^{5/2}}{64}\cdot\frac{e}{\sqrt{m}}\cdot\frac{\sqrt{n}}{1}\cdot\frac{1}{E_F^2}\,. \tag{2}$$

Giuliani and Quinn extended the Fermi-Liquid theory to the case of 2D-systems [10]. Their conclusions are based on theoretical work by A.V. Chaplik [11], M.J. Uren et al. [12], and E. Abrahams et al. [13]. They found a lifetime dependence for excited electrons in a 2D system of the following form:

$$\tau_{ee}^{-1} = \tau_0^{-1}\cdot(E-E_F)^2\ln\left|E-E_F\right| \tag{3}$$

In comparison to the 3D case, the inelastic lifetime τ_{ee} shows an additional logarithmic dependence of the excitation energy. This is the result of the competing effect of the planar geometry and the conservation of energy and momentum during the electronic collision processes. Furthermore, they emphasized the interesting point, that τ_{ee} does not depend on the electric charge. This is a consequence of the screening by the Coulomb potential. In contrast, in a 3D system τ_{ee} depends on the electric charge e (see eq. 2).

The quasiparticle behavior in a 1D-system (e.g. nano-wires), especially its inelastic lifetime, was calculated by M. Luttinger [14]. He found that the scattering rate increases linearly with increasing excitation energy:

$$\tau_{ee}^{-1} = \tau_0^{-1}\cdot\left|E-E_F\right| \tag{4}$$

Therefore, the inelastic lifetime of the quasiparticles in a one-dimensional surrounding follows a hyperbolic $1/|E\text{-}E_F|$ curve.

Figure 2 shows a plot of the energy dependence of τ_{ee} in a 3D, 2D, and a 1D metal without considering the unknown material dependent prefactor τ_0^{-1}.

As expected the reduced phase space for electron-electron scattering events at lower dimension points towards an increased lifetime. But please notice that the prefactor τ_0^{-1} is not included in these theoretical plots, which can considerably change the lifetime ratio between the 3D, 2D and 1D results at certain excitation energies $E - E_F$.

In this paper we will focus on the change of the electron dynamics by a transition from 3D to 2D. We continually reduced the thickness of an ultrathin silver film on a HOPG (highly oriented pyrolitic graphite) substrate and studied the change of the inelastic lifetime τ_{ee} of optically excited electrons.

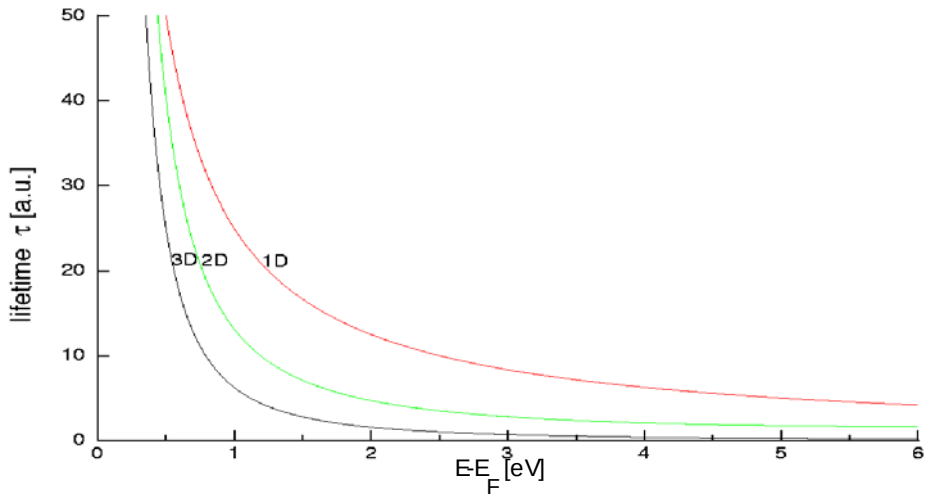

Figure 2. Schematic comparison of the predicted energy dependence of the inelastic lifetimes of excited electrons in a 3D, 2D, and in a 1D system.

3.2. PLASMON EXCITATION IN NANOPARTICLES

In mesoscopic systems the dynamical properties of optically excited electrons are not only altered due to the reduced phase space for scattering events but rather how the light is adsorbed in the system. In metal nanoparticles, collective electronic oscillations, so-called Mie-plasmons, can be excited by light and are, therefore, detectable as a pronounced optical resonance in the visible or UV parts of the spectrum. In recent years, several linewidth measurements and time resolved SHG autocorrelation measurements on metallic (Au, Ag) nanoparticles have been published, reporting a dephasing time T_2 (also often called decay or damping time) of the localized particle plasmon excitation in the order of 6-10fs [15, 16, 17].

Much less is known about the physical mechanism underlying the dephasing time T_2. The following mechanisms are possible, depending on the size, size distribution, shape, and dielectric constant of the surrounding medium: First, the plasmon can decay by pure dephasing, e.g. a decay of the fixed phase correlation between the individual electronic excitations of the whole oscillator ensemble, described by a pure dephasing time T_2^*. Common discussed mechanisms are scattering on surfaces or simple decay of the collective mode due to inhomogeneous phase velocities caused by the spread of the excitation energy or the local inhomogeneity of the nanoparticles. Second, the plasmon can also decay due to a transfer of energy into quasi-particles (electron-hole pairs) or reemission of photons (radiation damping and luminescence), described by $T_1 \equiv \tau_{ee}$.

We focus on the study of elliptically-shaped silver nanoparticles with axes of 40 nm by 80 nm and a height of 45 nm. Silver nanoparticles are of particular interest as they can exhibit particularly strong size-dependent optical extinction in the visible

spectral range (1.8 eV – 3 eV) due to resonantly driven electron plasma oscillations. Elliptically-shaped metal nanoparticles show two different plasmon resonances, which lie at different wavelengths for light polarized parallel to the short and long axes, respectively (see Figure 3).

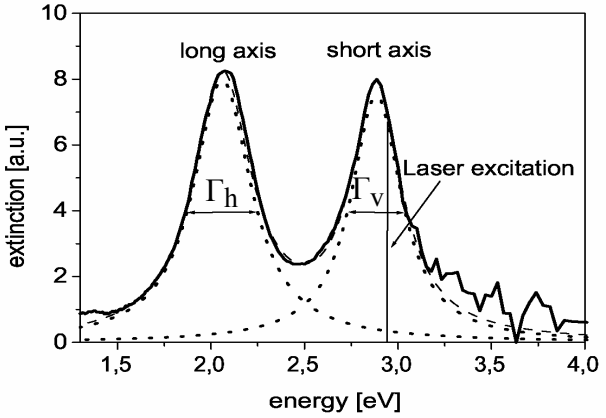

Figure 3. Measured extinction spectrum of the nanoparticle array. The low- and high-frequency peaks correspond to the Mie-plasmon, excited along the long and short axes of the elliptical Ag particles, respectively.

Tuning the laser wavelength to one of these two resonances allows distinguishing between resonance excitation and off-resonance excitation by simply changing the polarization of the laser pulse. Please notice that in both cases the excitation is the result of an intraband process, since the excitation energies of the Mie-plasmons in those silver nanoparticles lie below the interband transition threshold (~ 4 eV). Consequently, the absorption cross-section in the visible region is dominated by Drude damping [18]. The contribution due to interband transitions is negligible.

The excited electronic system in large nano-particles (>10nm) can exhibit additional dominant microscopic relaxation channels that are not important in bulk materials, such as radiation damping. Compared with Drude damping the radiation damping is explicitly frequency dependent. In this paper we concentrate on the question whether the same microscopic damping processes (due to photons, phonons, impurities, surface scattering, and electron-electron interactions) are involved when the photoexcitation is close to the Mie-plasma resonance or far from it.

4. The experiments

4.1. TIME-RESOLVED TWO-PHOTON PHOTOEMISSION (TR-2PPE)

The experimental method used to investigate the lifetime of optically excited electrons in a metal is the time-resolved two-photon photoemission (TR-2PPE). This method is known to be a highly accurate method to determine the dynamics of hot electrons in

unoccupied and occupied states. The pump-probe technique enables a direct measurement of the dynamical properties in the time domain with a resolution in the

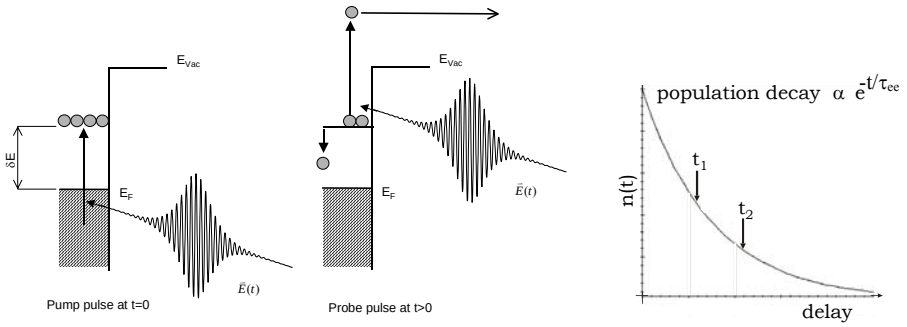

Figure 4. Principal mechanism of the time-resolved two-photon-photoemission (TR-2PPE) and the temporal behavior of the population N(t) in the intermediate state.

range of few femtoseconds [6]. The principle is schematically shown in Figure 4. A pump pulse excites electrons out of the valence band into usually unoccupied states with energies between the Fermi and vacuum level. A second probe pulse subsequently photoemits the excited electrons. The photoemission yield depends on the transient population of these intermediate states as a function of the temporal delay of the probe pulse with respect to the pump pulse. The measured pump-probe-signal contains information on the energy relaxation time T_1 of the population in the intermediate state, as well as its dephasing time T_2.

The experiments were performed with a femtosecond Kerr lens mode-locked Ti:sapphire laser (Tsunami, SpectraPhysics), pumped by a cw-operated diode pumped solid state laser ($Nd:YVO_4$, Millennia X, SpectraPhysics). The system delivers transform-limited and $sech^2$ temporal shaped pulses with up to 12 nJ/pulse, a duration of 20 fs – 40 fs at a repetition rate of 82 MHz and a wavelength of 780-830 nm. The linearly polarized output of the Ti:sapphire laser has been frequency-doubled in a 0.2 mm thick beta-barium-borate (BBO) crystal in order to produce UV pulses at about $h\nu = 3.0$ eV corresponding 415 nm. In a Mach-Zehnder-interferometer the pulses are divided by a beamsplitter into equal intensity (pump and probe) pulses. Hereby one path is delayed with respect to the other by a computer-controlled delay stage. Both beams were combined collinearly by a second beamsplitter and focused onto the sample surface. The diameter of the laser spot on the sample is around 100 µm. The plane of polarization can be rotated by means of a half wave plate to any arbitrary angle.

The samples were held in an ultra-high vacuum chamber at a base pressure in the 10^{-10} mbar range. A bias of U = –4 V was applied to the sample to eliminate the effects of any stray electric fields. The photoemitted electrons were detected in a cylindrical sector analyzer (CSA, Focus GmbH). The entrance axis of the energy analyzer is 45°

with respect to the laser beam. In general, we used a pass energy of 4 eV, leading to roughly $\Delta E = 50$ meV resolution.

4.2. SAMPLE PREPARATION

The ultrahin Ag films were grown onto a HOPG substrate, using an e-beam evaporator at a rate of about 0.1 ML/s, controlled by a pre-calibrated microbalance. Note that one monolayer (1 ML) silver corresponds to a height of 2.045 Å. The base pressure while evaporation was in the 10^{-9} mbar range.

The nanoparticle samples were produced in the group of Professor Aussenegg, Karl-Franzens University in Graz. The two-dimensional array of nearly identical, parallel oriented silver particles are deposited lithographically on a transparent ITO substrate, which itself lies on a glass plate [19]. Figure 5 depicts a SEM picture, and Figure 6 illustrates the geometry, size and the distances of the particles in the array.

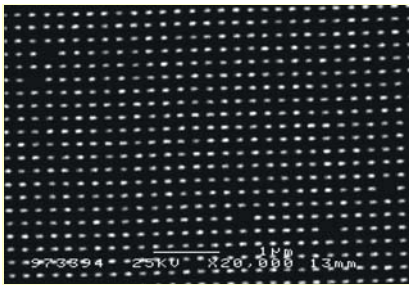

Figure 5. SEM picture of lithographically fabricated nano-particles on ITO

As particle shape and interparticle distances can be varied independently, this method allows us to tailor the optical properties of single particles. Thus the resonance frequency and the strength of particle interactions can be changed separately. Thereby the optical extinction maximum can be tuned to the desired wavelength, e.g. to our illuminating laser wavelength of 415 nm.

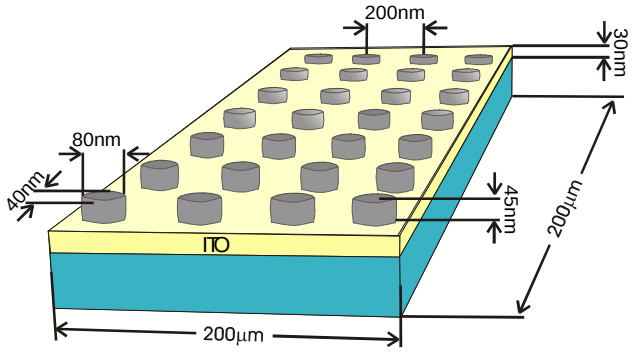

Figure 6. Array of silver-nanoparticles deposited on ITO

Figure 3 shows the two different resonances in the extinction spectrum at $\omega_a = 2.1$ eV and $\omega_b = 2.95$ eV for both axes, respectively. Liebsch's predictions that the Mie-plasmon damping is nearly independent of the resonance frequency [20] are in good agreement with the measured linewidth of the peaks in the extinction spectrum. For the long axis, $\Gamma_a = 0.4$ eV and for the short axis, $\Gamma_b = 0.39$ eV are observed.

In the following, the long axis of the elliptic particle is called 'v' and the short axis is called 'h'.

5. Results and discussion

5.1. ELECTRON DYNAMICS IN ULTRATHIN SILVER FILM ON HOPG

The relaxation of photoexcited electrons in ultrathin Ag-films at an energy of $E-E_F = 1.24$ eV is shown in Figure 7. Above 25 ML a small reduction in the lifetime τ with increasing film thickness is observed, caused by an increasing transport effect as discussed in [21]. The transport of the photoexcited electrons away from the surface region adds to the system-intrinsic decay due to inelastic scattering and reduces the measured lifetime with respect to the actual one. This transport effect is diminished and finally even eliminated by using films as thin as the penetration depth of the laser light within the investigated material.

For thinner films (<25 ML) a completely anomalous behavior is observed. The lifetime increases from about 25 fs at 25 ML to almost 40 fs at 15 ML silver. The data seem to match the intuitive assumption that the dynamics of the electron relaxation process should differ as soon as the thickness of the metal film becomes smaller than the mean free path of the excited electrons. The electronic structure of metallic thin films grown on a substrate is very different from that of the corresponding bulk crystal. The continuous bands split up into discrete energy levels due to quantum size effects (QSE). This electron confinement should result in a decreased phase space for electron-electron scattering events and, hence, in an increase of the inelastic lifetime τ_{ee} of the optically excited electrons.

An additional increase in the lifetime τ_{ee} is expected at even lower film thickness (< 15ML) due to the transition from a 3D-bulk to a 2D-system as shown in Figure 2. However, the measured data in Figure 7 show a decrease in τ_{ee} at lower coverage.

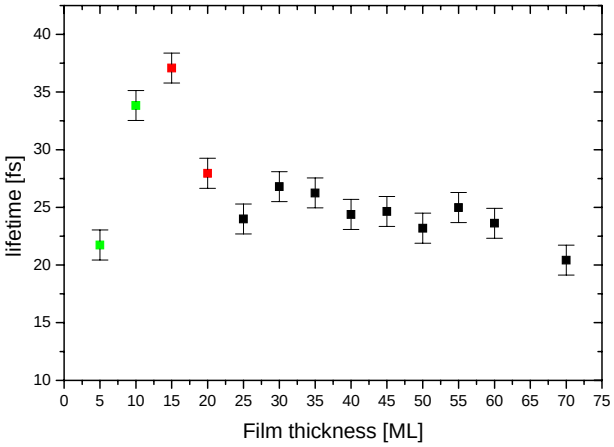

Figure 7. Film thickness dependence of silver on HOPG, at E-E_F = 1.24 eV. It is clearly visible that there is a levelling off at thicker layers, and a dramatic change in the region, where the system changes from 3D to 2D.

Atomic force microscopy (AFM) measurement revealed that the growth mode of silver on is not regularly or even epitactic. The images show a clear tendency to metal clustering below 20 ML. Nevertheless, also small metal clusters should give rise to QSE and cannot explain the observed decrease in the lifetime τ. The reduction in τ can be explained by the fact that the lifetime measurements at lower silver coverage (0 - 15 ML) are influenced by an increasing number of photoexcited electrons from the uncovered HOPG areas. Additional measurements on clean HOPG in the investigated excitation energy range (E-E_F > 1.0 eV) showed a very rapid (< 5 fs) relaxation of the photoexcited electrons. This explanation for the reduction of the lifetime τ below 15 ML is confirmed by the measured change of the work function with increasing Ag thickness as shown in Figure 8.

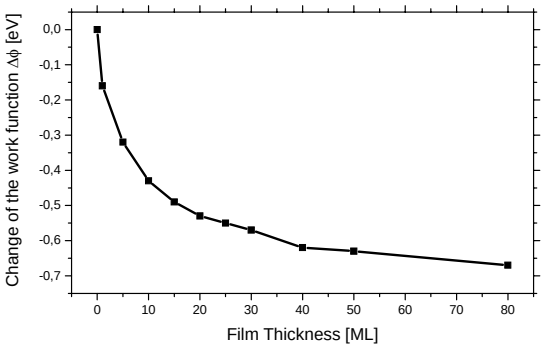

Figure 8. The change of the work function from pure HOPG via small layer thicknesses to an 80 ML silver layer.

The work function difference between HOPG and a thick Ag film is about 0.7eV. But as presented in Figure 8 the drop of the work function does not happen within a few ML of Ag as expected by an uniformly grown silver film. Therefore, it is assumed that the decrease of the lifetime τ at thicknesses below 15 ML is rather caused due to the increasing number of photoexcited electrons of the clean HOPG surface than due to the transition from 3D-bulk to a 2D layered structure.

To summarize our results on ultrathin Ag "films": The data show a clear change of the dynamics of optically excited electrons as soon as the nominal thickness of the metal film becomes smaller than the mean free path of the excited electrons. In order to obtain a quantitative picture of the change of the dynamics by the transition from 3D-bulk to a 2D layered structure, a more uniform grown thin film on a dielectric substrate (e.g. MgO) is required. Further investigations in this project are in progress.

5.2. THE LIFETIME DIFFERENCE OF MIE-PLASMONS AT AND OFF-RESONANCE

Let us now examine the electron relaxation in the silver nanoparticles, deposited as an array on an ITO substrate. Figure 9 shows the photoemission yield as a function of the polarization angle of the laser pulse. Clearly visible is the strong enhancement in the 2PPE yield in the case of a resonant plasmon excitation (denoted by 'h') compared to off-resonant excitation (denoted by 'v'). The shapes of the 2PPE photoemission spectra, however, do not show distinct differences by an excitation in the 'v' or 'h' direction (not shown). The resonant enhancement of the photoemission yield can be explained by the enlarged absorption of light by an extinction in the 'h' direction and by the lightning rod effect [22] meaning that the field enhancement can occur simply due to a concentration of the electric field at positions of maximum curvature (tip effect).

Figure 10 shows the FWHM determined from the autocorrelation traces of the TR-2PPE measurement as a function on the polarization angle of the incoming light. Each data point is represented by the FWHM of a sech^2-shaped curve fitted into the autocorrelation measurement. A typical autocorrelation measurement is shown in the inset.

For comparison reference autocorrelation traces of polycrystalline tantalum were measured at an intermediate state energy $E\text{-}E_F = 2.8$ eV. In this energy range, the lifetime of excited electrons in a transition metal is less than 1 fs [6] and hence, the traces obtained for tantalum represent the pure laser autocorrelation. The FWHM data for tantalum do not depend on the polarization angle of the incoming light. Therefore, any effect caused by an increase of dispersion due to rotation of the half wave plate can be excluded.

As one can see the FWHM is reduced from almost 75 fs in the ‘h’ direction (short-axis mode, resonant plasmon excitation) to 69 fs in the ‘v’ direction (long-axis mode, off-

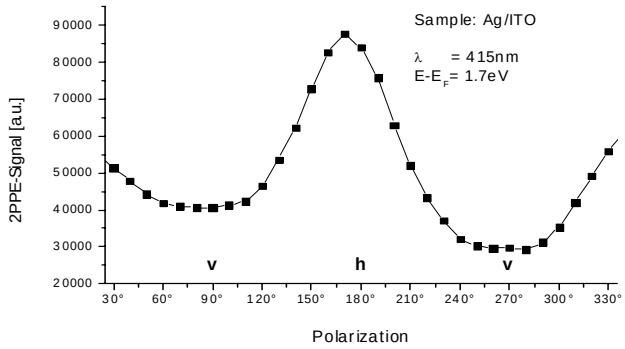

Figure 9. 2PPE yield versus polarization of the incident blue light. In case of the plasmon excitation (‘h’) a strong rise in the 2PPE-signal occurs.

resonant plasmon excitation). Further rotation of the polarization restores the long lifetime of the resonant Mie-plasmon excitation case. Please note that these FWHM values still include the autocorrelation of the laser pulse width. One can clearly see a difference in the FWHMs between resonance and off-resonance. This observation points unambiguously to a different electron dynamics.

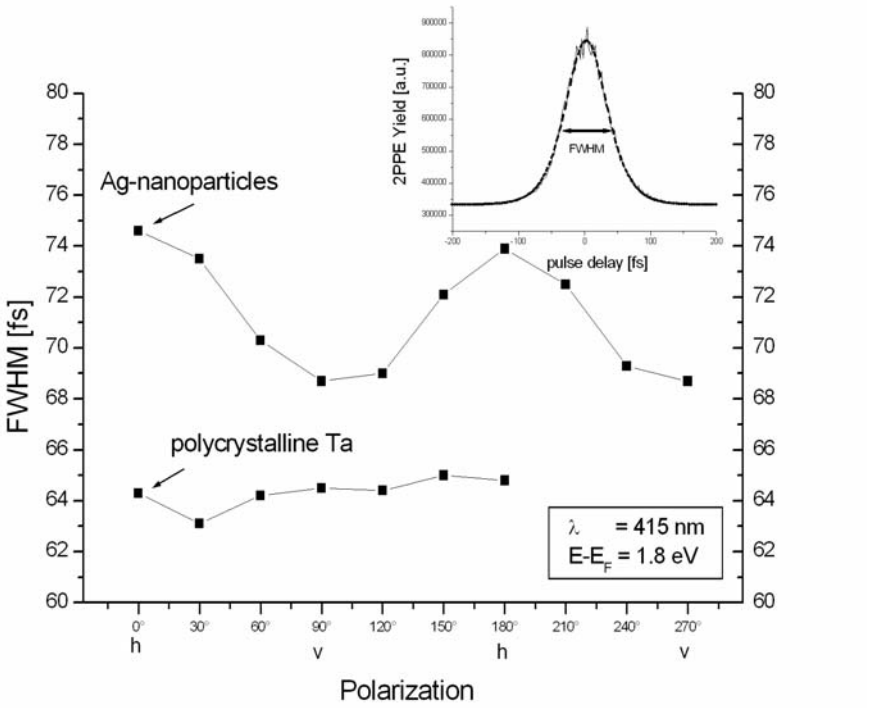

Figure 10. Nano-particles show a variation of the FWHM of the autocorrelation over rotating states of light polarization while tantalum shows no effect. In the inset, a typical autocorrelation measurement can be seen from which the data points have been derived.

It might be tempting to conclude that on-resonance collective excitation in general have a longer lifetime than excitation far from resonance. According to Liebsch *et al.* [20], the different damping rates obtained under on- and off-resonance conditions, as shown in Figure 10, can also be explained by different magnitudes of radiation damping along the short and long axis of the elliptical particles. This result is consistent with the fact that for spherical particles, radiation losses become more pronounced with increasing radius. Surface scattering plays a role only at radii less than about 5 nm. Moreover, Liebsch's theory predicts that collective plasma oscillations within the nano-particles are subject to the same microscopic Drude damping processes due to phonons, impurities, electron-electron interactions as off-resonance excitations [20]. None of these inelastic scattering mechanisms are reduced or absent if the electrons oscillate near the resonance excitation. However, the theory also points out that for an excitation, which matches the low frequency peaks in the extinction spectrum (Mie plasmon excited along the long axes) the radiation damping leads to a longer lifetime at off-resonance than at resonance.

In summary, it was demonstrated that the specific structuring of the material on a nanometer scale can govern the effective electron dynamics. In particular for defined silver ellipsoids the off-resonance excitation lifetime can be shorter or longer than the lifetime at resonance, depending on the incidence conditions of the laser light and on the dimensions of the metallic nanoparticles.

6. Acknowledgements

We are grateful to B. Lamprecht, H. Ditlbacher, J. R. Krenn and F. R. Aussenegg for providing us with many Ag-nanoparticle samples. We would like to thank M. Bauer and A. Liebsch for valuable discussions. This work was supported by the Deutsche Forschungsgemeinschaft (DFG).

7. References

1. Haight R. (1995) Electron Dynamics at Surfaces, *Surface Science Reports* **21**, 275-325
2. Schmuttenmaer C.A., Aeschlimann M., Elsayed-Ali H.E., Miller R.J.D., Mantell D., Cao J., and Gao Y. (1994) Time resolved Two Photon Photoemission from Cu(100): Energy Dependence of Electron Relaxation, *Physical Review B.* **50**, 8957
3. Hertel T., Knoesel E., Wolf M., and Ertl G. (1996) *Physical Review Letters* **76**, 535
4. Aeschlimann M., Bauer M., Pawlik S., Weber W., Burgermeister R., Oberli D., Siegmann H.C. (1997) Ultrafast spin-dependent electron dynamics in fcc Co, *Physical Review Letters* **79**, 5158
5. Petek H. and Ogawa S. (1997) *Progress in Surface Science* **56**, 239
6. Aeschlimann M., Bauer M., and Pawlik S. (1995) Femtosecond Time-Resolved Measurement of Electron Relaxation at Metal Surfaces, *Physical Chemistry* **99**, 1504
7. Ohms T., Porath R., Scharte M., Beesley J., and Aeschlimann M. (to be published) Electron spin dynamics in a GaAs/metal interface

8. Ferell R. A. (1956), *Physical Review* **101,** 554

9. Quinn J. (1963), *Applied Physics Letters* **2**, 167

10. Giuliani G.F. and Quinn J. (1982) Lifetime of a quasiparticle in a two-dimensional electron gas, *Physical Review B* **26**, 442

11. Chaplik A.V. (1971), Sov. Phys. – JETP **33**, 997

12. Uren M.J., Davies R.A., Kaveh M. and Pepper M. (1981), *Journal of Physics C* **14**, L395

13. Abrahams E., Anderson P.W., Lee P.A. and Ramakrishnan T.V. (1981) Quasiparticle lifetime in disordered two-dimensional metals, *Phys. Rev. B* **24**, 6783

14. Luttinger J.M. (1961) Analytic Properties of Single-Particle Propagators for Many-Fermion Systems, *Physical Review* **121**, 942

15. Lamprecht B., Leitner A., and Aussenegg F.R. (1999), *Applied Physics B* **68**, 419

16. Vartanyan T., Simon M., and Träger F. (1999), *Applied Physics B* **68**, 425

17. Klar T., Perner M., Grosse S., von Plessen G., Spirkl W., and Feldmann J. (1998), *Physical Review Letters* **80**, 4249

18. Ashcroft N.W. and Mermin N.D. (1976) *Solid State Physics*, Holt, Philadelphia

19. Gotschy W., Vonmetz K., Leitner A., Aussenegg F.R. (1996), *Optic letters* **21**,1099

20. Scharte M., Porath R., Ohms T., Aeschlimann M., Krenn J.R., Ditlbacher H., Aussenegg F.R., Liebsch A. (2001) Do Mie plasmons have a longer lifetime on resonance than off resonance? *Applied Physics B* **73**, 305-310

21. Aeschlimann M., Bauer M., Pawlik S., Knorren R., Bouzerar G., Bennemann K. H. (2000) Transport and dynamics of optically excited electrons in metals, *Applied Physics A* **71,** 5, 485-491

22. The lightening rod effect means that the field enhancement can occur simply due to a concentration of the electric field at positions of maximum curvature (tip effect)
Wokaun A. (1984) *Solid State Physics, p.223*, Ehrenreich H., Thurnbull T., and Seitz F. (Editors), Academic, New York